Optically induced carrier transfer in silicon anti-modulation-doped GaAs/$Al_xGa_{1-x}As$ single quantum wells

C.I. Harris, B. Monemar,* G. Brunthaler,† and H. Kalt
Max-Planck-Institut für Festkörperforschung, D-7000 Stuttgart 80, Federal Republic of Germany

K. Köhler
Fraunhofer Institut für Angewandte Festkörperphysik, D-7800 Freiburg, Federal Republic of Germany
(Received 22 April 1991)

A series of single-quantum-well samples doped with Si in the well (antimodulation), has been investigated using photoluminescence and photoluminescence excitation spectroscopy. The photoluminescence spectra are found to show a strong dependence on the excitation photon energy, in particular as it is increased above the $Al_xGa_{1-x}As$ band gap. This effect is interpreted in terms of transfer to the well of free carriers photogenerated in the barrier material. The band bending in the system implies that only photoexcited electrons are transferred into the well; the resulting charge separation creates an internal field that strongly alters the confining potential of the quantum well. A dual-excitation technique allows us to control independently the potential, and probe the resulting electronic structure of the quantum well. Measurements made with picosecond-time-resolved spectroscopy also highlight the importance of free-exciton capture at impurities in the presence of an electric field. A model for the carrier-transfer process that accounts for the excitation energy threshold at the $Al_xGa_{1-x}As$ band gap is discussed.

I. INTRODUCTION

The optical properties of quantum-well (QW) structures are strongly influenced by the presence of dopant impurities in either the well or barrier material.[1] As a result intentional doping provides a powerful tool in the design of quantum systems for device applications[2] or for research into specific confinement effects. Fundamental research has in particular focused on modulation-doped structures with their potential for the direct study of many-body theory effects.[3–6] However, the situation for which the impurity is present in the well and not in the barrier (anti-modulation-doped), has received less attention despite the important implications for quantum devices. The possible effects of the impurity within the well are manifold: it can provide carriers for conduction, act as a scattering site—hence limiting mobility—or be important as a center for radiative or nonradiative recombination. Such properties have been extensively studied in bulk material; a multiple-layer structure brings, in addition, a spatial dependence to the properties of the impurity according to the interaction between the host material and its neighbors. An important aspect of the work presented here is to highlight the importance of the band-bending resulting from the transfer of charge from dopants in the well. The resulting distortion in the confining potential is found to play a significant role even at the lowest doping level. It is apparent that such possible effects in an unintentionally doped system should not be neglected.

To date there has been a significant amount of work, both theoretical and experimental, on the properties of isolated hydrogenic dopants in quantum wells; for a review see, for example, Masselink *et al.*[7] The high-doping limit, for which the interaction between impurities becomes significant (leading to band degeneracy at the extreme) has not yet been studied in any detail in a confined system (Refs. 8–10 make some contribution towards a theoretical treatment of such a system). In this same limit, the perturbation of the confining potential, which can result from a high concentration of ionized centers, can dominate the properties of the system. This point is more apparent for modulation-doped structures where impurities are usually in an intentionally ionized state. The possibility of an optically induced charge redistribution for an asymmetric modulation-doped system was demonstrated by Chaves *et al.*[11] and has also been studied by Delalande *et al.*[12] In this work we report on a strong optically induced charge transfer effect, which occurs in Si anti-modulation-doped GaAs-$Al_xGa_{1-x}As$ single quantum wells.

Samples have been investigated with low temperature photoluminescence (PL) and photoluminescence excitation (PLE) spectroscopy, using both a single- and a dual-light-source excitation technique. Transient PL spectroscopy has also been carried out to analyze the dynamics of carrier transfer in returning to an equilibrium charge distribution, typically on the ms time scale. Theoretical calculations based on a simple model accounting for the excitation intensity dependence of this process are presented and discussed.

Further measurements have been carried out using picosecond-time-resolved spectroscopy enabling a closer study of the recombination mechanisms taking place in

the well. A strong capture to donors is observed for the high-doped samples, which accounts in part for the relatively strong quenching of the exciton luminescence in PL in comparison to PLE. The strong capture model is further supported by temperature-dependent work in which we observe the reappearance of the quenched exciton at elevated temperatures.

The paper is arranged into separate sections which discuss each experiment and its contribution to our understanding of the overall model. Finally we make some conclusions and general remarks regarding further work.

II. EXPERIMENTAL PROCEDURE

The samples used in this investigation have been prepared using molecular-beam epitaxy (MBE) on a semi-insulating GaAs substrate. An initial wide GaAs buffer layer followed by a short-period superlattice have been grown in order to reduce the background carbon level. The QW structure itself consists of a single 100-Å GaAs well sandwiched between 300-Å $Al_{0.34}Ga_{0.66}As$ barriers (see Fig. 1). The growth temperature was chosen at 680 °C, for which segregation effects, which smear the doping profile in the growth direction, are minimized at the expense of poorer interface quality. The relatively wide central 50 Å of the well is Si doped to provide a large number of donor sites, the dopant being added concurrently without using interrupted growth. All the other layers in the structure are nominally undoped. Samples have been prepared with a range of doping levels from 2.5×10^8 cm^{-2} (essentially undoped) to 2.5×10^{12} cm^{-2} (above the degenerate limit). A detailed discussion of the specific changes in the PL spectra of doped QW's observed for increasing doping levels is given in Ref. 13. In the work presented here, results from two examples are discussed: a low-doped sample, 2.5×10^8 cm^{-2}, and a high-doped sample (but below the degenerate limit), 7.5×10^{11} cm^{-2}. The close proximity of the surface to the quantum well ($\sim$ 350 Å) implies a strong influence of surface states, the band bending imposed by the pinning of the Fermi level at the surface[14] will thus play a significant role in determining the properties of the system.

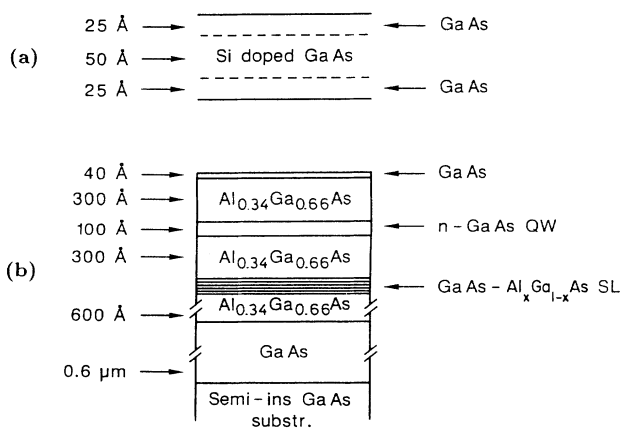

FIG. 1. Single $GaAs/Al_xGa_{1-x}As$ quantum-well structure under investigation; (a) shows the well doped in the central 50 Å, which is embedded in the layer sequence (b).

Time-integrated photoluminescence measurements have been carried out in the temperature range from 1.6 K up to room temperature. A number of different excitation sources were used to cover the energy range of interest: at "high" photon energy either by the 5145-Å (2.41 eV) line of the Ar^+-ion laser or at low intensity (up to 25 μW) by filtering the emission of a high-power xenon lamp through a 0.32-m monochromator. A tunable dye laser using LD700 dye and pumped using a Kr^+-ion laser was used to provide excitation in the longer wavelength range 7250–8050 Å (1.71–1.54 eV). The excited luminescence was focused onto the entrance slit of a Spex double monochromator and detected using a cooled GaAs cathode photomultiplier. Excitation spectroscopy has been made using the dye laser to scan the excitation in the range 7250–8000 Å.

Picosecond-time-resolved PL measurements have been carried out using a synchronously pumped, mode-locked dye laser with a repetition rate of 80 MHz and a pulse width of 5 ps. A Styryl 8 dye was used to give a tuning range from 7400 to 8100 Å and to allow resonant PL excitation. The luminescence was dispersed through a 0.32-m spectrometer and detected using a Hamamatsu streak camera giving the total luminescence as a function of both time and energy. The temporal resolution of the system is approximately 10 ps.

Further PL transient data have been measured using an acousto-optic modulator to provide excitation pulses of 10-ms duration, the luminescence being detected using a box-car photon-counting technique on the equipment described above. Luminescence decay in the ms time scale was measured.

III. RESULTS AND DISCUSSION

A. Photoluminescence under different photon energy excitation

The low-temperature steady-state photoluminescence spectra for two different samples at low- and high-doping levels are presented in Figs. 2(a) and 2(b), respectively. The results of excitation at high and low photon energy are contrasted. For the low-doped sample under high-energy excitation, we observe a typical single, strong exciton transition. Under lower energy excitation, the sample shows a significant downshift in energy of the main exciton peak and a second well-resolved peak at lower energy. The high-doped case under the same comparison of excitation conditions demonstrates a correspondingly more significant difference. Again at high-photon-energy excitation a single peak is observed; however, the low-energy excitation here results in an apparent total loss of excitonlike recombination and only a broad luminescence extending to lower energies is observed.

An estimate of the strength of the mechanism behind the observed variation in PL properties can be made from a dual-excitation experiment. Two excitation sources are

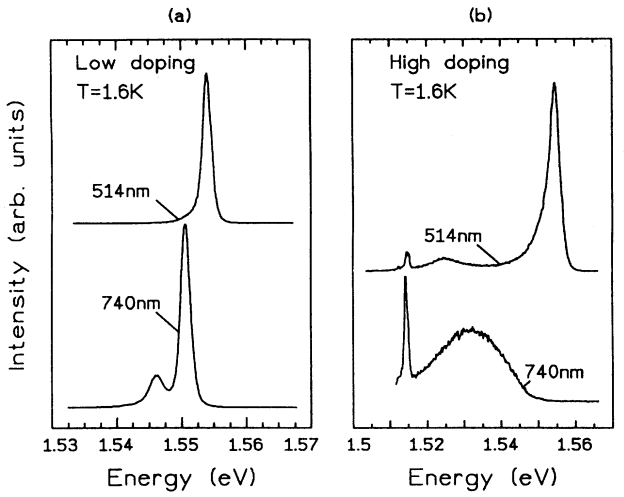

FIG. 2. Photoluminescence spectra for excitation at two different wavelengths; (a) the low-doped sample shows a distinct upshift in energy of the main exciton peak for excitation of higher energy, (b) the highly doped sample shows no exciton peak for low-energy excitation.

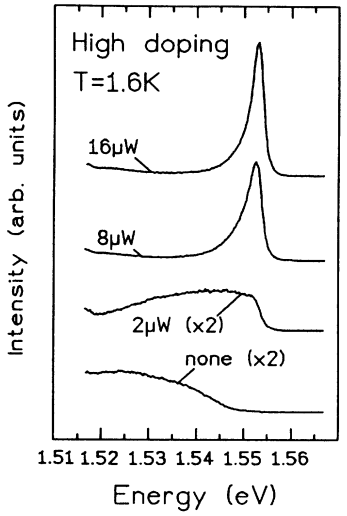

FIG. 3. Development in photoluminescence spectra in a dual excitation experiment for increasing intensity of the high-energy (2.1 eV) component (low-energy component constant at 0.1 W/cm^2). The highly doped sample illustrates a distinct transition from excitonic to broad-band recombination. The low-doped sample (not shown) demonstrates an equivalent transition between the two states illustrated in Fig. 2(a).

used to excite the sample in Figs. 3 and 4; in both cases the lower-photon-energy source is kept at constant energy and intensity while the high-photon-energy source is varied. The results of illumination with high photon energy of variable intensity are given in Fig. 3. Results will be discussed here for the high-doped case, but a corresponding transition between the limits of Fig. 2 can be shown for the low-doped sample. The necessary high-photon-energy intensity threshold to restore the excitonic character of the luminescence is of the order of a few μW/cm^2, compared to the 0.1 W/cm^2 typically used for the low-photon-energy intensity. We are thus observing a highly efficient activation of the process responsible for the observed transition to the case of excitonic PL spectra. Furthermore, if the photon energy of the low-intensity component is scanned, in this case using the xenon lamp filtered through a small monochromator, we observe a relatively abrupt transition to the "excitonic case" as the excitation energy is increased above the $Al_xGa_{1-x}As$ band gap (see Fig. 4). The implied mechanism is then dependent upon the generation of free carriers in the $Al_xGa_{1-x}As$ barrier material. The charge redistribution brought about by the transfer of this photogenerated charge into the well alters the local potential, given that the electron and hole become spatially separated in the process, i.e., only if one charge type transfers and not both. If both the electron and hole are transferred into the well, the two contribute to the total recombination, but do not affect the confining potential. Transfer of a single carrier type only must therefore occur.

The idea of carrier-induced optical effects through the introduction of carriers by optical excitation has been discussed in the context of many-body effects by a number of authors.[11,12,15] Under high-intensity excitation the resulting high-density electron-hole plasma brings about a band-gap renormalization due to correlation and exchange interaction.[16] The control of the two-dimensional electron density via optical excitation in a modulation-type doped structure has been considered by Chaves *et al.*[11] They observe a shift in the energetic position of a QW transition and interpret this as a change in the band

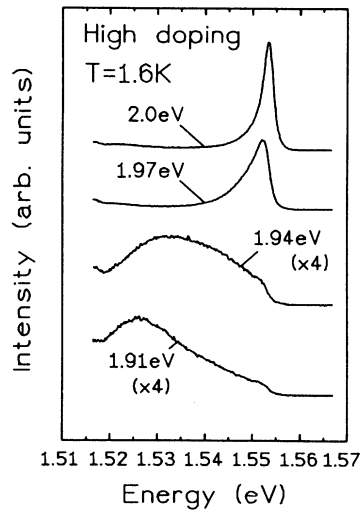

FIG. 4. Results of dual excitation experiment where the energy of the second component has been varied from below to above the barrier band gap (at constant 16 μW power, low-energy component approximately 0.1 W/cm^2). For increasing excitaton energy the exciton transition is enhanced.

bending and correlation energy of the system. Similarly Plaut *et al.*[17] have also observed a reduction in electron density under specific-photon-energy excitation in a single GaAs/$Al_xGa_{1-x}As$ heterojunction. The observation of the opposite effect, i.e., of decreasing electron concentration, corresponds to reversed band bending, which exists in the modulation-doped system. The effect of an induced change in the electron concentration in a quantum well on the optical spectra can be more readily observed by using a field-effect-transistor configuration;[18,19] such a system allows easy control of charge densities and has enabled detailed correlation of the optically observed many-body effects with carrier density.

In contrast to the majority of the systems described above, the QW structure under investigation here is antimodulation-doped and at low temperatures has essentially no free carriers (degenerate doping is not considered in this paper[13]). The role of many-body theory as applied to free carriers can therefore not be applied in the interpretation of the observed phenomena. The Fermi level for n-type doped samples will nominally reside at the donor level high in the band gap. The barrier material in this case is undoped; however, the dominant background impurity in $Al_xGa_{1-x}As$ is usually the carbon acceptor, hence the barriers are weakly p-type and as a result there is a certain amount of compensation between well and barrier. The structure is additionally complicated, however, by the close proximity of the surface. The high density of defect states at the surface pins the Fermi level at approximately 0.6 eV below the bulk-GaAs conduction band;[14] as a result there is a further transfer of charge to the surface and depletion of donors in the well at room temperature.[20] The equilibrium distribution of charge, therefore, results in band bending, which strongly distorts the confining potential of the system. Exactly what proportion of the donors is ionized is not easily deduced; however, it is clear that for the highest-doped samples (not shown here) there still exists a strong Moss-Burstein shift.[21] The limit on the depletion of the well (approximately 10^{18} cm^{-3}), which is apparent from the onset of band filling as the high-energy emission tail shifts to higher energies, is in good agreement with a simple calculation of the carrier density given that the internal field must align the Fermi level pinned at the surface with the subband edge in the well. On this basis it is reasonable to assume that the low doped wells are essentially totally depleted. A potential-energy diagram showing the band bending for the two cases is given in Fig. 5. In the next section we develop a model of charge transfer based upon the proposed band structure which accounts qualitatively for the results observed in emission spectra.

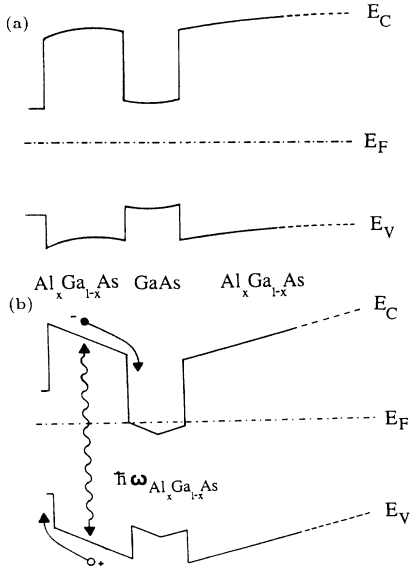

FIG. 5. Schematic diagram of the band structure of the single quantum-well samples for low (a) and high (b) doping. The close proximity of the surface implies a strong influence of the Fermi-level pinning due to surface states (Ref. 14).

B. Carrier-transfer model

Excitation at energies above the band gap of the $Al_xGa_{1-x}As$ barrier will result in the formation of free-electron-hole pairs. Under the influence of the internal field the charges are swept in opposite directions, the electron being drawn towards the well where it is trapped by a positively charged donor (Fig. 5), while the hole is lost to the surface or towards the substrate. At low temperatures this process of charge rebalance will continue, given sufficient photogenerated carriers, until flat-band conditions exist between well and barrier, i.e., no internal field across the well. The size of the internal field is dependent upon the number of ionized donors and therefore increases for higher doping (up to the depletion limit). At higher doping and hence high fields the exciton PL spectra are strongly perturbed.

The reason for the distinct threshold for carrier transfer associated with the barrier band gap is not immediately apparent. The high density of electrons bound at the Fermi level at the surface implies that it is possible even with low-photon-energy excitation to excite electrons with kinetic energy larger than the $Al_xGa_{1-x}As$ barrier (although momentum considerations imply a relatively low probability transition), and hence for them to move into the well under the influence of the internal field. Similarly, and as we shall argue later, an electron bound to a donor within the well can be excited with sufficient kinetic energy to escape the well. The dynamic equilibrium set up by these two processes is that observed under low-photon-energy excitation. The difference for $Al_xGa_{1-x}As$ excitation is interpreted in terms of the role of the photogenerated hole. The behavior of the hole in the $Al_xGa_{1-x}As$ in the adjacent layers above and below the well is not the same. An electron-hole pair generated in the near surface $Al_xGa_{1-x}As$ is rapidly spatially separated, the hole moving to the surface where it recombines with an electron. The surface reservoir of electrons due to defect states prevents an accumulation of holes at the expense of depletion. Holes generated in the $Al_xGa_{1-x}As$ layer below the well are swept towards the substrate; the absence of any electron "reservoir," however, means that the holes tend to accumulate and carrier transfer to the

well is rapidly reduced. We therefore propose that the dominant processes are taking place in the near surface region.

The influence of an externally applied field perpendicular to the well plane has been examined by a number of groups.[22–24] The work of Mendez *et al.*[24] demonstrated a reduction in PL intensity with increasing field, which they interpreted as due to the spatial separation of carriers within the well. The same work also noted, under low fields, a second peak in addition to the main exciton transition; this second peak is associated with the recombination of ground-state electrons with a carbon (acceptor) impurity (e, A). The presence of an electric field apparently then relatively enhances the free-to-bound transition.

In direct analogy to the external field case, we are able to make a similar interpretation of the results presented here in terms of the existence of an internal field. The presence of a static electric field will have multiple effects upon the exciton transiton energy:[23] (1) the effective band gap of the bulk semiconductor is reduced through tilting of the band edges, the Franz-Keldysh effect,[25] (2) the binding energy of the exciton (B_{ex}) will be modified by the relative difference in effect upon the motion of the electron and hole,[26] (3) the variation in confinement energies of the electron (E_e) and the hole (E_h) caused by the local distortion of the well.

The exciton transition energy is given then by

$$E_{ex1} = E_G + E_{h1} + E_{e1} - B_{ex1} \ . \quad (1)$$

The observed shift in the exciton transition with different excitation photon energies (Fig. 2) can be interpreted predominantly in terms of the latter two effects. The reduction in luminescent intensity leading to total quenching of the exciton in the high-doping case [Fig. 2(b)] with 740 nm can partly be explained as due to the spatial separation of the carriers in the well. The probability that the electron and hole recombine either directly or through first forming an exciton is reflected in the overlap of the respective wave functions. At zero field the wave functions are symmetric about the well center and their overlap is at a maximum. In general, in the presence of an electric field the distribution of electrons and holes is polarized in opposite directions; this reduces the wave-function overlap and the effective recombination probability. The polarization in carrier distribution is not equivalent for both carrier types and is relatively stronger for the heavy hole.[24] In the present case, the "sagging" potential of the high-doped sample illustrated in Fig. 5(b) has the effect of more strongly localizing the hole wave function at the edge of the well, while we interpret the effect on the electron distribution to be less extreme. The reduced overlap in electron-hole wave functions implies that a photoexcited electron has a greater chance to relax and be captured at an ionized donor site. As a result we observe under low-energy excitation and hence high fields what we believe is an enhanced donor to valence-band transition. It is difficult to make a definite assignment on the basis of comparison with calculated donor binding energies[27] since the local well potential is not well defined; the separation to the exciton peak ($\sim$ 2.7 meV) is, however, approximately consistent. A similar interpretation supports the assignment of Mendez *et al.*[24] of an acceptor-related transition under external field conditions.

C. Excitation spectroscopy measurements

The above internal field model is strongly supported by photoluminescence excitation spectroscopy measurements. Dual excitation has again been used to control the internal potential and probe the resulting structure. Figure 6 shows the development in excitation spectra for the highly doped sample under increasing intensity of the high-photon-energy component excitation, under comparable conditions to Fig. 3.

In the absence of any secondary excitation the n=1 heavy-hole-exciton resonance is strongly reduced while the light-hole-exciton strength is apparently unperturbed. For increasing illumination with high-energy excitation the heavy-hole exciton is recovered (Fig. 6). The shift in energy of the light-hole exciton between zero and saturation is some 4 meV, while for the heavy hole there is a significantly smaller shift. If we compare the shift in the light-hole exciton with the theoretical calculations of Brum and Bastard[22] the predicted field strength is greater than 100 kV cm^{-1}; a field of this magnitude is on the field-ionization limit of the heavy-hole exciton and may partly account for the strong reduction. It is not clear why there should be a reduced shift in the heavy-hole-exciton resonance; however, this may be an artifact of the changing potential shape to which it is strongly susceptible, as pointed out earlier. It is interesting to further note that there is effectively no perturbation of the n=2 exciton resonance or band edge. If indeed the observed shifts are due to changes in the electron and hole confinement energies then corresponding shifts should be observed for higher subbands. However,

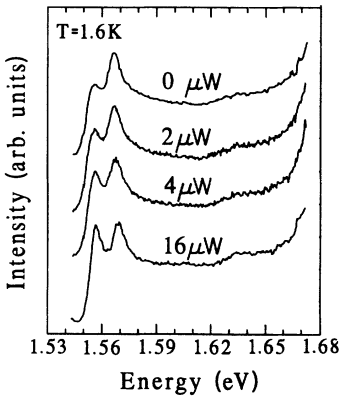

FIG. 6. Excitation spectra for the highly doped sample under increasing intensity of the additional high-photon-energy (2.0 eV) excitation component (low-energy component constant at 0.1 W/cm^2). The heavy-hole exciton is progressively recovered, and begins to dominate over the light hole at higher intensities due to scattering taking place in the well.

if the shifts are predominantly due to changes in exciton binding energy the effects for higher subbands are potentially much weaker, the latter case seems to be implied by our results. It is interesting to note that the observed exciton shift in excitation spectra is not reflected in photoluminesence. The Stokes shift in this system is therefore also dependent on the internal field, the larger Stokes shift occurring for larger field strengths. The implication of the internal field model described above is that under high-field conditions the hole wave function is compressed towards the edge of the well. Studies of the $Al_xGa_{1-x}As/GaAs$ interface[28] have highlighted the ability of well-width fluctuations (growth steps at interface forming monolayer islands) to localize carriers, in particular holes. The increased Stokes shift then follows the increased localization of the hole at the barrier-well interface.

D. Dynamics of carrier transfer

The transfer and subsequent return to equilibrium of carriers following a high-energy-excitation pulse have been studied using time-resolved photoluminescence spectroscopy on a ms time scale. An optoacoustic modulator has been used to provide low-intensity excitation pulses of a few ms duration; at the same time the sample is continuously excited with the low-photon-energy illumination (again the dual excitation procedure). The intensity of the pulsed excitation is typically a few μW, while the continuous illumination at low photon energy is considerably more intense, of the order of 1 mW or more. Figure 7 illustrates the sharp onset of exciton luminescence, corresponding to in-filling of carriers by the high-photon-energy pulse, and the subsequent spectral changes reflecting the slow relaxation of the potential as the carrier distribution returns to equilibrium under low-photon-energy excitation only.

Figure 8 shows the decay in luminescence as detected at the exciton transition. On the time scale investigated the onset of exciton character is essentially coincident with the beginning of the laser pulse. A strong dependence of the decay time upon the intensity of the low-energy excitation is found. Higher intensity results in more rapid decay. As a consequence of this dependence there is an apparent competition between the processes resulting from the different illumination energies, i.e., filling of electrons into the well and reexciting out of the well. In fact it is likely that the high-energy excitation induces both processes, but the in-filling of electrons is the more efficient mechanism in this case.

As a result of these two competing processes, we find that the maximum exciton PL intensity occurs at different times dependent on the low-energy intensity. Furthermore, the maximum occurs after the end of the filling pulse as a result of the exciton peak shifting down in energy with time. As we detect below, the maximum photon energy the peak energy relaxes through the detection point giving the false maximum observed initially in the decay curves (Fig. 8).

The idea of the intensity-dependent rebalance is an apparent contradiction to the proposed model of charge transfer from the $Al_xGa_{1-x}As$ barrier, since we have argued that a charge redistribution only occurs for the high-photon-energy excitation; we must, however, consider that following the in-filling of carriers there is a high density of electrons sitting on donor sites high in the band gap. Under illumination electrons are excited high into the conduction-band continuum (Fig. 9). Although the high-energy electrons rapidly relax back into the well, it is possible for a fraction of the electrons to transfer to the surface. We can consider from a statistical argument an average energy distribution of electrons at any instant in time. The exact form of the energy dis-

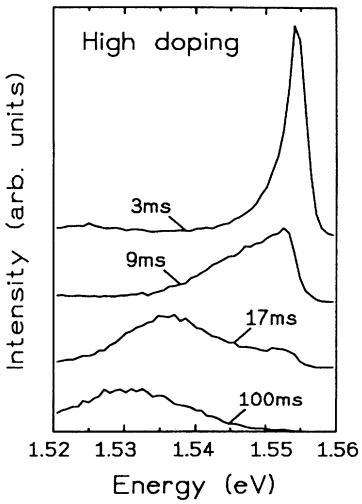

FIG. 7. Development of PL spectrum in time for a dual excitation experiment, where an optoacoustic modulator is used to produce pulses of 5-ms duration for the high-energy component. The low-photon-energy excitation is kept constant in this experiment at approximately 0.1 W/cm^2. The exciton transition is shown to decay on a time scale of approximately 100 ms.

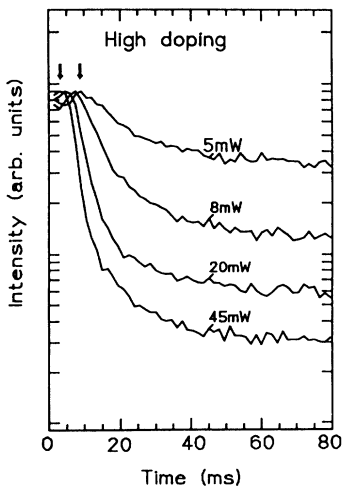

FIG. 8. Decay in PL as detected at the exciton transition. The decay rate is shown to be dependent on the low-energy illumination intensity for a fixed high-energy illumination.

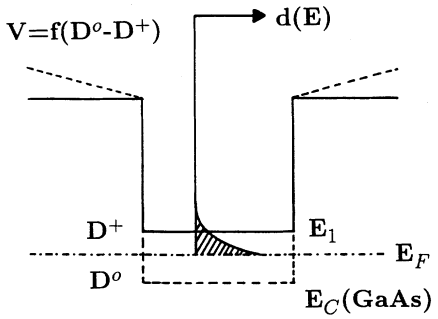

FIG. 9. Band diagram illustrating simplistic model with which we can interpret the dynamics of the observed decay in exciton luminescence following the high-energy excitation pulse. The carrier distribution is modeled by $d(E) = d_0 \times \exp[-(E - E_0)/kT_e]$, where T_e is the effective carrier temperature.

tribution of excited electrons will depend on a number of factors and cannot be treated simply in a realistic way. However, it is realistic to assume an exponential-type distribution which decreases rapidly at higher energies, and which can be characterized by a specific electron temperature T_e. Given a known distribution we can determine a transfer rate of electrons by considering both a tunneling component and also, by resolving the electron velocity perpendicular to the plane of the well, the direct transfer of electrons with sufficient kinetic energy. The barrier height presented to electron transfer is itself a function of the charge imbalance and increases as the system returns to equilibrium. As a result an iterative technique is used to calculate the decay in transfer. A derivation of the equations used in this basic analysis is given in the Appendix. The final governing equation (5) can be seen as a prefactor multiplied by a carrier-transfer probability, dependent on the total barrier height. Figure 10 shows the result of fitting to two of the decay curves. The calculated curve is a measure of how many nonequilibrium (i.e., imbalance from nonexcited distribution) electrons remain in the well and as such is not directly the measured quantity. In attempting to match the form of the decay we make the basic assumption that the exciton oscillator strength decreases linearly with increasing field. This relationship does not represent the actual dependence, but it allows some qualitative assessment to be made.[29] The aim of the simple model presented here is to demonstrate our ability to understand the gross features observed; the quality of the fit obtained allows some confidence in the picture presented. It is interesting to note that if we use the above results to calculate the field dependence of the oscillator strength we obtain a result qualitatively similiar to the work of Ref. 29.

E. Picosecond-time-resolved spectroscopy

The apparent total quenching in exciton luminescence in highly doped samples observed for excitation at low energy has been further investigated using picosecond-time-resolved spectroscopy. The lifetime parameters derived from measurements of this kind are important in understanding the mechanisms of the qualitative model described above. Figure 11 shows the spectral development of the high-doped sample resonantly excited at the n=2 exciton (1.66 eV).

Despite the absence of the exciton in the time-integrated spectra (Fig. 2), the exciton is strongly observed in time-resolved spectra during the excitation pulse. Following excitation, we observe a rapid capture of the exciton, here seen as an increasing rate of decay at higher energies as the exciton population is transferred to lower energies. The quenching of the exciton PL is in part then a consequence of the strong capture present in the system. A high capture probability is a simple reflection of the large number of capture sites available in the high-doped system. The exciton bound at the donor

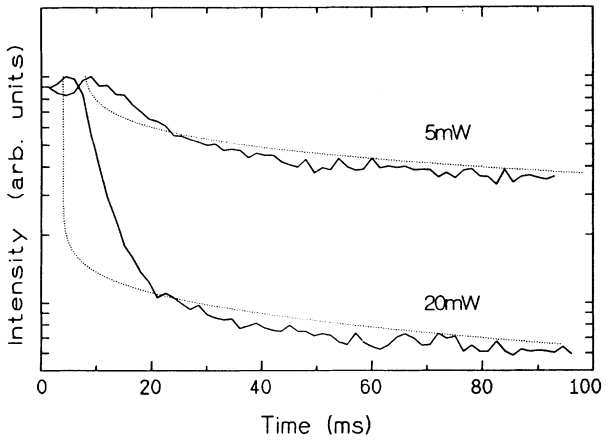

FIG. 10. Transients obtained with the carrier transfer model described in the text, matched to two of the measured decay curves. The ability to account for a decay of the form observed is demonstrated.

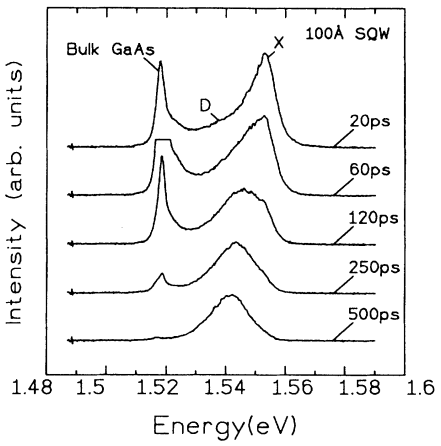

FIG. 11. Picosecond-time-resolved spectra demonstrating rapid spectral diffusion due to capture of free exciton at bound site followed by relaxation and break up of exciton to give slow decaying free-to-bound transition.

site (either neutral or ionized), we propose, is increasingly strongly localized finally being dissociated in the local field, leaving an electron bound at the donor and a spatially separated hole. As a result of this localization sequence, we observe at time >500 ps only the radiative decay of donor-bound electrons (D-band) in agreement with the time-integrated spectra.

The loss in exciton luminescence in the time-integrated spectra is a combination of two related effects, the polarization in carrier distributions leading to reduced oscillator strength and enhanced capture in the presence of a strong electric field. The mechanism behind enhanced capture, we propose, is predominantly a statistical one; the larger extension of the exciton wave function implied by reduced binding energy means that the number of possible capture sites enveloped is increased. Furthermore, enhanced capture may be associated with the relatively higher concentration of ionized donors under high-field conditions, for which the Coulombic potential gives an additional capture mechanism. The observed shift in the light-hole exciton indicates a field strength consistent with strong reduction in the oscillator strength. However, the picosecond data suggest a predominant role played by capture in quenching the exciton luminescence. The relative contribution of the two effects is difficult to assess due to their interdependence.

F. Temperature-dependent analysis

The importance of capture stressed above has been further examined by investigation of the temperature dependence of luminescence in the highly doped sample. Figure 12 illustrates the change in luminescence with increasing temperature in the range 8–200 K under single excitation at low photon energy (740 nm). Significantly, we observe at temperatures above 50 K a sudden reappearance of the exciton transition. In our previous analysis, the occurence of the exciton in the luminescence spectra has been associated with a change in the local well potential. However, it is unclear why a significant change in potential should result singularly from an increase in temperature. The large impurity binding energy [E_D=12 meV (Ref. 30)] associated with the strong confinement of the system implies that the effect of thermal ionization upon carrier concentrations at this temperature should be minimal. We propose that the observed effect is one of reduced capture at the donor. At elevated temperatures the exciton is less able to be localized to form a bound exciton.[30] If as suggested field ionization of the exciton does not take place, the reduction in exciton localization results in enhanced free-exciton recombination. This proposal is further supported by picosecond-time-resolved data, which indicates slower capture for increasing temperature.

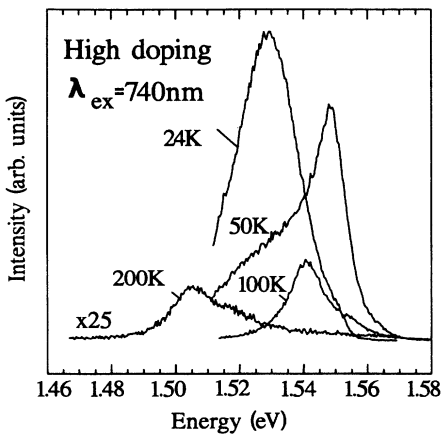

FIG. 12. Temperature dependence of PL spectra for highly doped sample under low-photon-energy excitation. The exciton transtition is recovered above 50 K, which is interpreted as a reduction in the strong capture demonstrated in Fig. 11.

IV. CONCLUSIONS

The importance of doping in perturbing the local potential in a single quantum well has been demonstrated. Perturbation of the confining potential results from superposition of the Coulombic field associated with the ionized impurities on the band profile. The dopants become ionized due to compensation with background impurities (in particular, the carbon acceptor present in MBE growth), or by charge loss to surface or interface states. We have observed spectra consistent with the neutralization of the Coulombic field when free carriers are photogenerated in the $Al_xGa_{1-x}As$. The internal field has an increasingly strong effect as the concentration of dopants is increased. In direct analogy to the case of an externally applied field we observe a reduction in the exciton binding energy and oscillator strength for increasing field. We have also discussed a simple model based on the idea of neutralizing the ionized donors which is able to account for the general features observed in the time-resolved spectra. Picosecond-time-resolved data along with temperature-dependent measurements have further shown that capture by ionized impurities is apparently enhanced relative to the neutral species. A direct result of this is that at high doping concentrations the perturbation of the band structure coupled with strong capture is able to totally quench the exciton luminescence. If the impurities are neutralized by optical generation and subsequent transfer of free carriers, the exciton is recovered in the luminescence spectra. Dependent on the optical excitation energy we have an effective two-state system. Measurements on a ms time scale following a high-photon-energy pulse have further demonstrated that once the impurities are neutralized they remain neutral at low temperatures for long periods. On the basis of these initial results it is possible to consider applications of this mechanism in a totally optical switching element, using the ability of a high-photon-energy pulse to flip the output state of an element and for it to remain in that state for time intervals in the fraction of a second range. Further theoretical work is needed to provide more quantitative support of the ideas put forward here.

ACKNOWLEDGMENTS

The authors would like to express their thanks to Dr. Jörg Weber for useful discussion and W. Heinz for technical assistance.

APPENDIX

The calculation of the loss in photoexcited carriers from the well follows the assumption that the relative number of electrons with a given kinetic energy at any instant is expressed by a simple Boltzmann type distribution (see Fig. 9). This distribution is then characterized by an effective carrier temperature T_e, which is one of the two parameters used to model the carrier flux, the other being the initial field (V_i) present following the excitation pulse.

We assume a distribution of the form

$$d(E) = d_0 e^{-(E-E_0)/kT_e} , \tag{A1}$$

where d_0 is a normalization coefficient derived by considering that the sum over all states must represent the total number of excited carriers. E_0 is the zero-point energy, i.e., the boundary between excited and nonexcited electrons, in this case the Fermi level E_F.

The number of excited carriers in a given energy range dE is thus given by

$$dn = g(E)d(E)dE . \tag{A2}$$

For simplicity in calculation we assume the density of states to be three dimensional but taking the band edge to correspond to the first subband in the quantum well. This gives

$$dn = \left(\frac{1}{2\pi}\right)^2 \left(\frac{2m^*}{\hbar^2}\right)^{3/2} (E - E_1)^{1/2} \frac{1}{kT_e} \times e^{-(E-E_F)/kT_e} dE . \tag{A3}$$

We consider two possible mechanisms for the carrier escape, (1) direct thermal transfer and (2) tunneling through the barrier. Due to the barrier width the second component was found to be negligible and thus only the thermal component will be discussed.

The kinetic energy of the excited electron is given by the difference $E - E_1$. We now substitute for this energy difference and resolve the velocity perpendicular (V_x) and parallel (V_y, V_z) to the barrier. We assume that only those electrons traveling towards the barrier with kinetic energy in excess of the total barrier height are transferred. The total barrier height will be a function of the $Al_xGa_{1-x}As$-GaAs conduction-band offset E_{BO}, the position of the Fermi level in the well, and the effective internal field (V) due to the charge imbalance. Integrating over those electrons above the minimum velocity for transfer and then substituting for the total barrier height gives us an equation for the particle flux:

$$J = dn\, V_x = \left(\frac{m^*}{\hbar^3}\right) \left(\frac{kT_e}{2\pi^2}\right) e^{-(qV+E_{BO})/kT_e} . \tag{A4}$$

The internal field V we calculate on the basis of charge imbalance distributed over a two-dimensional sheet. The conduction-band offset E_{BO} has been taken as 60% of the total band-gap difference. Our final equation (5) essentially represents a prefactor multiplied by a transfer probability. This probability is dependent on the total barrier height as would be intuitively expected.

*Permanent address: Department of Physics and Measurement Technology, Materials Science Division, Linköping University, S-58183 Linköping, Sweden.

†Current address: Johannes Kepler University, A-4040 Linz, Austria.

[1] C. Delalande, Physica **146B**, 112 (1987).

[2] D.A.B. Miller, D.S. Chemla, T.C. Damen, A.C. Gossard, W. Wiegmann, T.H. Wood, and C.A. Burrus, Appl. Phys. Lett. **45**, 13 (1984).

[3] G.E. Bauer and T. Ando, Phys. Rev. B **31**, 8321 (1985).

[4] S. Schmitt-Rink, C. Ell, and H. Haug, Phys. Rev. B **33**, 1183 (1986).

[5] M.H. Meynadier, J. Orgonasi, C. Delalande, J.A. Brum, G. Bastard, M. Voos, G. Weimann, and W. Schlapp, Phys. Rev. B **34**, 2482 (1986).

[6] A. Pinczuk, J. Shah, H.L. Störmer, R.C. Miller, and W. Wiegmann, Surf. Sci. **142**, 492 (1984).

[7] W.T. Masselink, Y.-C. Chang, H. Morkoc, D.C. Reynolds, C.W. Lother, K.K. Bajaj, and P.W. Yu, Solid State Electron. **29**, 205 (1986).

[8] N. Holonyak, Jr., B.A. Voyak, H. Morkoc, T.J. Drummond, and K. Hess, Appl. Phys. Lett. **40**, 658 (1982).

[9] A. Gold, J. Serve, and A. Ghazali, Phys. Rev. B **37**, 4589 (1984).

[10] U. Ekenberg, Phys. Rev. B **30**, 3367 (1984).

[11] A.S. Chaves, A.F.S. Penna, J.M. Worlock, G. Weimann, and W. Schlapp, Surf. Sci. **170**, 618 (1986).

[12] C. Delalande, J. Orgonasi, M.H. Meynadier, J.A. Brum, G. Bastard, G. Weimann, and W. Schlapp, Solid State Commun. **59**, 613 (1986).

[13] C.I. Harris, B. Monemar, H. Kalt, and K. Köhler, Phys. Rev. B (to be published).

[14] A. Chandra, C.E.C. Wood, D.W. Woodward, and L.F. Eastman, Solid State Electron. **22**, 645 (1979).

[15] G. Tränkle, H. Leier, A. Forchel, H. Haug, C. Ell, and G. Weimann, Phys. Rev. Lett. **58**, 419 (1987).

[16] R. Cingolani, H. Kalt, and K. Ploog, Phys. Rev. B **42**, 7655 (1991).

[17] A.S. Plaut, I.V. Kukushkin, K.V. Klitzing, and K. Ploog, Phys. Rev B. **42**, 5744 (1990).

[18] H. Yoshimura, G.E.W. Bauer, and H. Sakaki, Phys. Rev. B **38**, 10791 (1988).

[19] C. Delalande, J. Orgonasi, J.A. Brum, G. Bastard, M. Voos, G. Weimann, and W. Schlapp, Appl. Phys. Lett. **51**, 1346 (1987).

[20] E.F. Shubert, J.M. Kuo, R.F. Kopf, A.S. Jordan, H.S. Luftman, and L.C. Hopkins, Phys. Rev. B **42**, 1364 (1990).

[21] T.S. Moss, Proc. Phys. Soc. London Sect. B **76**, 775 (1984); E. Burstein, Phys. Rev. **93**, 632 (1954).

[22] J.A. Brum and G. Bastard, Phys. Rev. B **31**, 3893 (1985).

[23] T.H. Wood, C.A. Burrus, D.A.B. Miller, D.S. Chemla, T.C. Damen, A.C. Gossard, and W. Wiegmann, Appl. Phys. Lett. **44**, 16 (1984).
[24] E.E. Mendez, G. Bastard, L.L. Chang, L. Esaki, H. Morkoc, and R. Fischer, Phys. Rev. B **26**, 7101 (1982).
[25] L.V.Keldysh, Zh. Eksp. Teor. Fiz **34**, 1138 (1958) [Sov. Phys. JETP **7**, 788 (1958)]; W. Franz, Z. Naturforsch. **13a**, 484 (1958).
[26] D.S. Chemla, T.C. Damen, D.A.B. Miller, A.C. Gossard, and W. Wiegmann, Appl. Phys. Lett. **42**, 864 (1983).
[27] M. Stopa and S. DasSarma, Phys. Rev. B **40**, 8466 (1989).
[28] M.H. Meynadier, J.A. Brum, C. Delalande, M. Voos, F. Alexandre, and J.L. Lievin, J. Appl. Phys. **58**, 4307 (1985).
[29] Jia-Lin Zhu, Dao-Hua Tang, and Jia-Jiong Xiong, Phys. Rev. B **39**, 8609 (1989).
[30] D.C. Reynolds, C.E. Leak, K.K. Bajaj, E.E. Stuty, R.L. Jones, K.R. Evans, P.W. Yu, and W.M. Theis, Phys. Rev. B **40**, 4156 (1989).